

Differential requirements for clathrin in receptor-mediated endocytosis and maintenance of synaptic vesicle pools

Ken Sato^{a,1}, Glen G. Erntrom^b, Shigeki Watanabe^b, Robby M. Weimer^b, Chih-Hsiung Chen^c, Miyuki Sato^a, Ayesha Siddiqui^c, Erik M. Jorgensen^b, and Barth D. Grant^{c,1}

^aLaboratory of Molecular Traffic, Institute for Molecular and Cellular Regulation, Gunma University, Maebashi, Gunma, 371-8512, Japan; ^bHoward Hughes Medical Institute and the Department of Biology, University of Utah, Salt Lake City, UT 84112-0840; and ^cDepartment of Molecular Biology and Biochemistry, Rutgers University, Piscataway, NJ 08854

Edited by Iva S. Greenwald, Columbia University, New York, NY, and approved November 26, 2008 (received for review September 28, 2008)

Clathrin is a coat protein involved in vesicle budding from several membrane-bound compartments within the cell. Here we present an analysis of a temperature-sensitive (ts) mutant of clathrin heavy chain (CHC) in a multicellular animal. As expected *Caenorhabditis elegans chc-1(b1025ts)* mutant animals are defective in receptor-mediated endocytosis and arrest development soon after being shifted to the restrictive temperature. Steady-state clathrin levels in these mutants are reduced by more than 95% at all temperatures. Hub interactions and membrane associations are lost at the restrictive temperature. *chc-1(b1025ts)* animals become paralyzed within minutes of exposure to the restrictive temperature because of a defect in the nervous system. Surprisingly synaptic vesicle number is not reduced in *chc-1(b1025ts)* animals. Consistent with the normal number of vesicles, postsynaptic miniature currents occur at normal frequencies. Taken together, these results indicate that a high level of CHC activity is required for receptor-mediated endocytosis in nonneuronal cells but is largely dispensable for maintenance of synaptic vesicle pools.

Caenorhabditis elegans | synapse

Clathrin is thought to promote vesicle formation at several steps in membrane trafficking (1). Clathrin forms a triskelion, composed of 3 heavy and light chains. Interactions between triskelia drive coat formation, with interdigitation of triskelia creating repeating hexagonal and pentagonal units (2). According to this model, clathrin is a key component of vesicle formation; specifically, it provides a template that can drive membrane curvature. In the presynaptic membranes of neurons, it has been proposed that clathrin-mediated endocytosis maintains synaptic vesicle pools (3, 4). The definitive test for this model is to assay synaptic vesicle formation after eliminating clathrin function by mutation. Unfortunately, loss of clathrin heavy chain (CHC) is embryonically lethal in metazoans (5, 6), precluding assays of presynaptic function in such mutants. A solution to the chronic lethality of clathrin mutants is to analyze temperature-sensitive (ts) alleles of the protein in which the effects of acute loss of the protein function can be analyzed. In this work, we analyze a ts allele of CHC in an animal and demonstrate a differential requirement for clathrin in receptor-mediated endocytosis in oocytes and the maintenance of synaptic vesicle pool in neurons.

Results

rme-3 Encodes *Caenorhabditis elegans* Clathrin Heavy Chain. Analysis of 2 endocytosis mutants, *rme-3(b1024)* and *rme-3(b1025ts)*, identified in our previous genetics screens, demonstrated that they are alleles of the only CHC gene in *C. elegans* (*chc-1*) (6). The oocytes of these mutants fail to endocytose a GFP-tagged yolk protein, YP170-GFP. In wild-type animals, YP170-GFP is cleared efficiently from the body cavity by yolk receptors expressed on the surface of oocytes (Fig. 1A). In *chc-1(b1024)* animals uptake of YP170-GFP was reduced significantly, resulting in the accumulation of YP170-GFP in the body cavity (Fig.

1B). *chc-1(b1025ts)* exhibited a ts defect in yolk uptake with variable uptake at the permissive temperature and uniformly blocked uptake at the restrictive temperature (Fig. 1C and D and data not shown). *chc-1(b1025ts)* mutant animals also arrested development soon after being shifted to the restrictive temperature [supporting information (SI) Fig. S1].

chc-1(b1024) contains a 3-kb Tc5 transposable element inserted within the predicted promoter region of *chc-1*, 292 bases upstream of the predicted start codon (Fig. 1E). In *chc-1(b1025ts)*, we identified a 9-bp deletion centered around the stop codon of the *chc-1* gene. This lesion results in the deletion of the C-terminal methionine, a residue that is identical in worm, mouse, and human CHC. Furthermore, the loss of the stop codon is predicted to result in an extension of the ORF, adding 22 novel amino acids to the C terminus. Thus, this allele of *chc-1* is similar to ts yeast CHC mutants in which the C terminus is deleted or altered (7, 8). The C-terminal region of CHC projects from the vertex of the triskelion and interacts with neighboring triskelia in clathrin lattices (9). The loss of the terminal methionine and the addition of 22 amino acids is likely to interfere with triskelion interactions (Figs. S2 and S3) (9).

Recent reports indicate that clathrin light chain (CLC) is not required for endocytosis but rather contributes to other clathrin-mediated trafficking steps (10). Consistent with these reports, we found that wild-type worms depleted of *C. elegans* CLC (CLIC-1) by RNAi displayed normal YP170-GFP endocytosis and animal viability (Fig. S1 H and I). However, RNAi of *chc-1* in the *chc-1(b1025ts)* mutant background at the permissive temperature of 15°C resulted in fully penetrant embryonic lethality, indicating that CLC does contribute to at least one clathrin-mediated function in vivo (Fig. S1I).

Endogenous CHC Protein Is Severely Reduced in the *chc-1(b1025ts)* Mutant. In wild-type oocytes, endogenous CHC is localized largely to small punctate structures associated with the plasma membrane of oocytes, as expected for clathrin localized to coated pits and vesicles (Fig. 2A–B'). In *chc-1(b1025ts)* oocytes, CHC protein was barely detectable and lacked cortical enrichment (Fig. 2C–D'). α -Adaptin is one of the components of the adaptor protein 2 complex that participates in the formation of clathrin-coated vesicles, as well as in the selection of cargo molecules for incorporation

Author contributions: K.S., E.M.J., and B.D.G. designed research; K.S., G.G.E., S.W., R.M.W., C.-H.C., M.S., A.S., and B.D.G. performed research; A.S. contributed new reagents/analytic tools; K.S., G.G.E., S.W., R.M.W., M.S., E.M.J., and B.D.G. analyzed data; and K.S., G.G.E., E.M.J., and B.D.G. wrote the paper.

The authors declare no conflict of interest.

This article is a PNAS Direct Submission.

¹To whom correspondence may be addressed. E-mail: sato-ken@showa.gunma-u.ac.jp or grant@biology.rutgers.edu.

This article contains supporting information online at www.pnas.org/cgi/content/full/0809541106/DCSupplemental.

© 2009 by The National Academy of Sciences of the USA

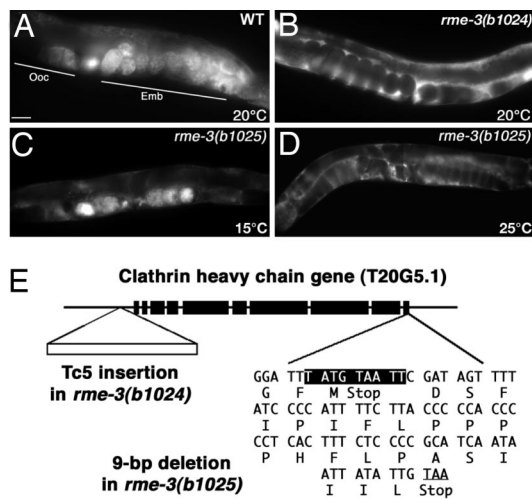


Fig. 1. *rme-3* encodes *C. elegans* CHC. (A–D) YP170-GFP endocytosis by oocytes of adult hermaphrodites. (A) In wild type, YP170-GFP is taken efficiently up by oocytes (Ooc) and after fertilization is found in embryos (Emb). (Scale bar, 30 μ m.) (B) In *rme-3(b1024)* mutants, very little YP170-GFP is endocytosed by oocytes; instead, YP170-GFP accumulates in the body cavity. (C) In *rme-3(b1025ts)* mutants, YP170-GFP uptake is mildly reduced in oocytes at 15°C. (D) At 25°C YP170-GFP uptake is blocked, and most YP170-GFP remains in the body cavity in *rme-3(b1025ts)* mutants. (E) In *rme-3(b1024)* a Tc5 transposable element is present in the *chc-1* promoter. In *rme-3(b1025ts)*, there is a 9-bp deletion spanning the stop codon. Black boxes indicate exons of *chc-1*.

into such vesicles (11). Like clathrin, α -adaptin is localized to small puncta on the plasma membrane of oocytes (Fig. 2 E and F). However, α -adaptin was enriched further in cortical puncta in *chc-1(b1025ts)* mutant oocytes, as has been observed previously when endocytosis is blocked in other organisms (Fig. 2 G and H) (12). Consistent with the localization data, anti-CHC-1 Western blots displayed strongly reduced band intensity at 15°C (4.5% of wild-type CHC) and 25°C (2.0% of wild-type CHC), suggesting that CHC-1 expression or stability is strongly impaired (Fig. 2I). Transgenic expression of GFP-tagged CHC-1(b1025) replicated the anti-CHC-1 immunofluorescence results (Fig. S2); the tagged mutant form of the protein expressed at an abnormally low level compared with wild-type controls and at the restrictive temperature failed to localize correctly to the plasma membrane in the gonad, intestine, and synaptic regions of neurons (Figs. S2 and S4 A–D’).

We also sought to examine the effects of the *b1025* mutation on clathrin assembly. The C-terminal one-third of CHC is often referred to as the “hub domain.” This region of CHC is necessary and sufficient for clathrin self-assembly into triskelia and also provides the binding interface for CLC (13). In a yeast 2-hybrid assay, wild-type CHC hub domains (residues 1075–1680) interacted with one another strongly both at 30°C and 37°C (Fig. S3). *b1025* mutant hub domains interacted with one another more weakly than wild-type hubs at 30°C and displayed a further weakened interaction at 37°C, suggesting that the *b1025* mutation tends to impair clathrin assembly, especially at higher temperatures (Fig. S3). These results suggest that the 2–5% of CHC remaining in *chc-1(b1025ts)* mutants is probably conditionally defective in assembly, a prerequisite for its association with membranes and endocytic vesicle formation. We note, however, that the permissive and restrictive temperatures for *C. elegans* are lower than those of yeast, so some caution is required in extending these interpretations to the *in vivo* situation in the worm.

CHC Is Concentrated in Presynaptic Regions of the Neuron. Particularly high rates of endocytosis are thought to be required at synapses to regenerate synaptic vesicles (14). Synaptic vesicle endocytosis is,

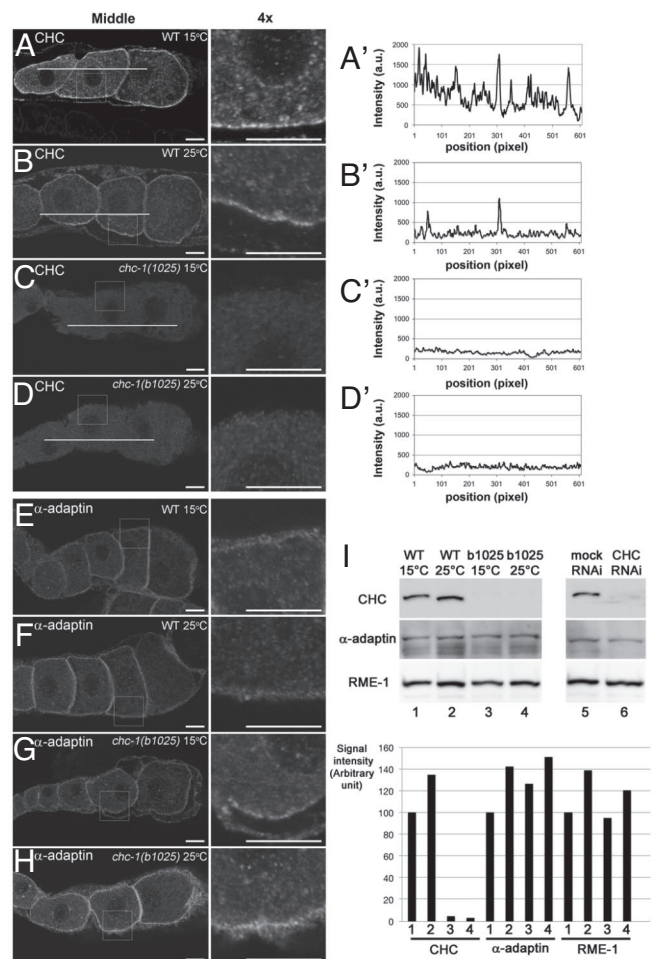


Fig. 2. Endogenous CHC levels are severely reduced in the *chc-1(b1025ts)* mutant. Gonads were dissected and immunostained with anti-CHC-1 (A–D) and anti- α -adaptin (E–H) antibodies. (A, E) wild type, 15°C; (B, F) wild type, 25°C; (C, G) *chc-1(b1025ts)*, 15°C; (D, H) *chc-1(b1025ts)*, 25°C. (A–H) Middle planes (Left) and enlarged images ($\times 4$) of boxed regions in the middle planes (Right) are shown. (Scale bar, 10 μ m.) (A’–D’) Fluorescence intensity of CHC staining as a function of position was graphed along a line through the center of the oocytes. (I) CHC protein level is dramatically reduced in *chc-1(b1025ts)* mutant animals. Total lysates were prepared from the indicated strains and were probed with anti-CHC, anti- α -adaptin, and anti-RME-1 antibodies in Western blots. Each lane is numbered. The signal intensity of each protein band was quantified and graphed (Bottom).

at least in part, mediated by clathrin, because synaptic vesicle components copurify with clathrin (4), and because clathrin-coated pits can be observed at synapses in electron micrographs (3). We analyzed clathrin localization *in vivo* in transgenic worms expressing mRFP (monomeric red fluorescent protein)-CHC in GABA neurons. mRFP-CHC was enriched in puncta in the neuronal processes with significant spatial overlap with GFP-synaptobrevin (GFP-SNB-1), a synaptic vesicle marker, demonstrating localization of CHC to the presynaptic varicosities *in vivo* (Fig. 3A–A’). We further analyzed GFP-CHC localization in neurons by immunostaining of GFP-CHC-expressing neurons with anti-SYD-2 (synaptic defective-2) antibodies. SYD-2/liprin is an active zone component that is required for active zone morphology and function (15). GFP-CHC-labeled puncta generally were adjacent to but not directly overlapping with structures labeled for SYD-2 (Fig. 3 B–B’), suggesting that clathrin-dependent endocytosis occurs in a region of the synapse distinct from, but adjacent to, the active zone. This result is in agreement with clathrin localization in the nervous system of other organisms (16).

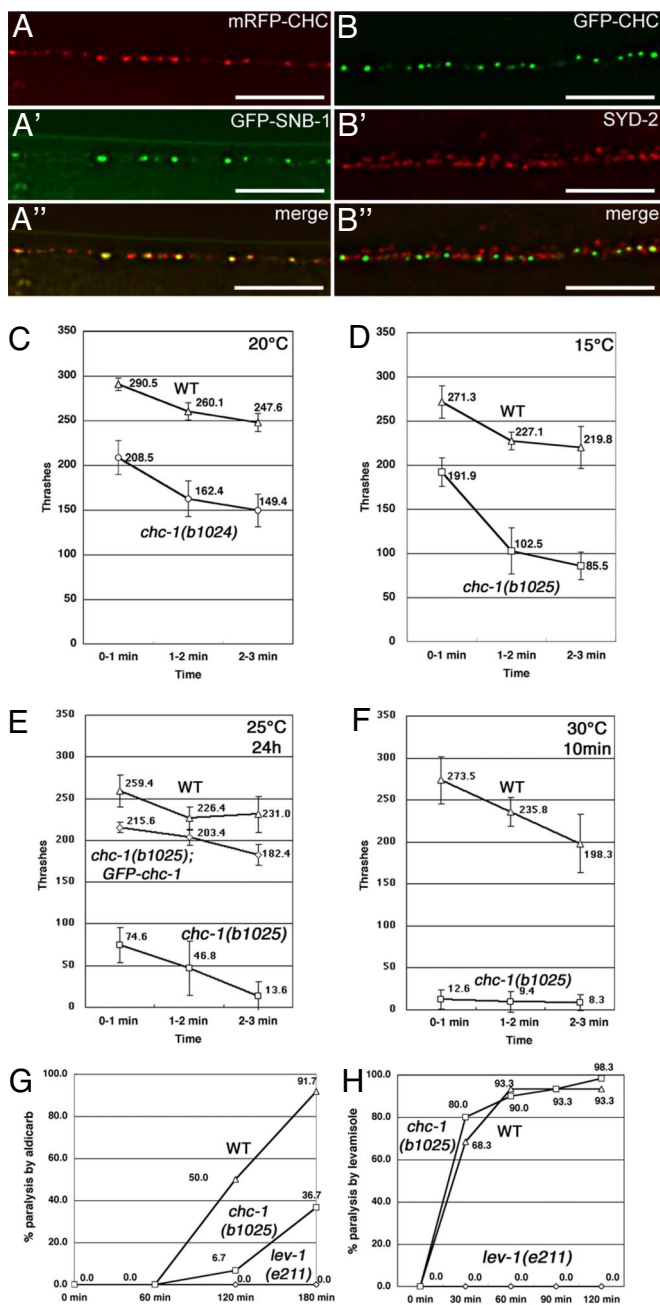


Fig. 3. Clathrin is required for neuromuscular function. (A–B'') CHC is concentrated presynaptically but is excluded from the active zone. (A–A'') Live worms co-expressing mRFP-CHC (A, A'') and the synaptic vesicle protein GFP-SNB-1 (A', A'') in GABA neurons were examined by fluorescence microscopy. (B–B'') Transgenic animals expressing GFP-CHC (B, B'') in the GABA neurons were stained with anti-GFP and anti-SYD-2 antibodies. Note that anti-SYD-2 antibody labels active zones in all synapses of the nerve cord (B'), whereas GFP-CHC labels only synapses in GABA motor neurons (B). (Scale bars, 10 μ m.) (C–F) Thrashing assays. (C) Wild-type L4 hermaphrodites ($n = 8$) and *chc-1(b1024)* ($n = 8$) were incubated at 20°C for 24 h and then transferred to M9 buffer. Head thrashes were counted. (D) Wild-type L4 hermaphrodites ($n = 8$) and *chc-1(b1025ts)* mutants ($n = 8$) were incubated at 15°C for 24 h and examined. (E) Wild-type L4 hermaphrodites ($n = 5$), *chc-1(b1025ts)* ($n = 5$), and *chc-1(b1025ts)* mutant animals expressing GFP-CHC (*dkEx6* [*P_{rgef-1}::GFP::chc-1*]) under the control of a neuron-specific promoter ($n = 5$) were incubated at 25°C for 24 h before examination. (F) Wild-type young adult worms ($n = 4$) or *chc-1(b1025ts)* mutants ($n = 8$) were incubated at 30°C for 10 min and examined. (G) Aldicarb resistance. Thirty young adult hermaphrodites of the wild type, *chc-1(b1025ts)*, and *lev-1(e211)* were placed on aldicarb plates (0.5 mM) at the semi-permissive temperature of

Clathrin Is Required for Neuromuscular Function. To assess aspects of synaptic function in clathrin mutants at the level of behavior, we analyzed swimming. When placed in a drop of buffer, normal worms perform rapid body bends with a reproducible periodicity. When we transferred wild-type worms to buffer, they continued thrashing actively for 3 min with only a slight decrement in rate (triangle, Fig. 3 C–F and *SI Text* and *Movie S1*). The weak mutant *chc-1(b1024)* thrashed at a slightly decreased rate compared with the wild type (circles, Fig. 3C). At the permissive temperature of 15°C, *chc-1(b1025ts)* worms also exhibited reduced thrashing activity compared with the wild-type control worms but continued to thrash slowly after 3 min (squares, Fig. 3D). After incubation at 25°C for 24 h, *chc-1(b1025ts)* animals initially displayed strongly reduced thrashing behavior and became almost completely paralyzed after 3 min, suggesting a progressive loss of synaptic function (squares, Fig. 3E, and *Movie S2*). We also observed a defect in pharyngeal pumping behavior in *chc-1(b1025ts)* animals consistent with defective neuronal function (Table S1).

To determine whether the thrashing defects in *chc-1(b1025ts)* animals were neuronal in origin, we expressed GFP-CHC under the control of a panneuron- (*rgef-1*) or muscle-specific promoter. *rgef-1* (F25B3.3) encodes the *C. elegans* orthologue of a Ca^{2+} -regulated ras guanine nucleotide exchange factor (*rgef-1*), which is expressed throughout the nervous system in *C. elegans* (17). The neuronal transgene restored the thrashing behavior of *chc-1(b1025ts)* animals to almost wild-type levels, indicating that most of the defects observed were caused by the reduced function of clathrin in the nervous system and not the musculature (diamonds, Fig. 3E). Expression of GFP-CHC in muscle did not improve the phenotype (data not shown). Expression of GFP-CHC-1(b1025) mutant protein in neurons did not complement the thrashing defect of the *chc-1(b1025ts)* animals and did not affect thrashing rates of wild-type animals, suggesting that the protein does not interfere with wild-type clathrin function (Fig. S4E). To determine whether there is an acute defect in synaptic transmission in *chc-1(b1025ts)* mutants, we raised worms at 15°C and then shifted them to 30°C for 10 min. Indeed, the defect was acute, because even this short exposure to restrictive temperature produced a significant thrashing defect in *chc-1(b1025ts)* animals compared with wild type (Fig. 3F). It is also possible that clathrin dysfunction unmasks an intrinsic temperature sensitivity of endocytosis or some other aspect of neurotransmission as reported for *ehs-1/eps15* deletion mutants (18).

As an additional test of whether *chc-1(b1025ts)* mutants have defects in pre- or postsynaptic transmission, we measured sensitivity to aldicarb and levamisole. Aldicarb is an inhibitor of acetylcholine esterase and causes a toxic accumulation of secreted acetylcholine at neuromuscular synapses (19). Aldicarb toxicity can be ameliorated by mutations that decrease neurotransmitter release at the synapse or that reduce the response to acetylcholine postsynaptically. *chc-1(b1025ts)* animals were less sensitive to aldicarb than wild-type worms, a phenotype that could be reversed by neuron-specific GFP-CHC expression (Figs. 3G and 5E). We also measured sensitivity to levamisole, an acetylcholine receptor agonist in nematodes (20). Levamisole sensitivity is thought to be purely postsynaptic. We found no significant difference in sensitivity to levamisole between the wild-type and *chc-1(b1025ts)* animals (Fig. 3H). We also found no significant difference in the postsynaptic muscle whole-cell membrane currents and resting membrane potential

22°C and checked for their ability to move at the indicated time-points in response to prodding. *lev-1(e211)* mutants that lack a subunit of the muscle inotropic ACh receptor were resistant to both aldicarb and levamisole and used as a control. (H) Levamisole sensitivity of *chc-1(b1025ts)*. Thirty young adult hermaphrodites of the wild type, *chc-1(b1025ts)*, and *lev-1(e211)* were placed on levamisole plates (60 μ M) and assayed for movement in response to prodding.

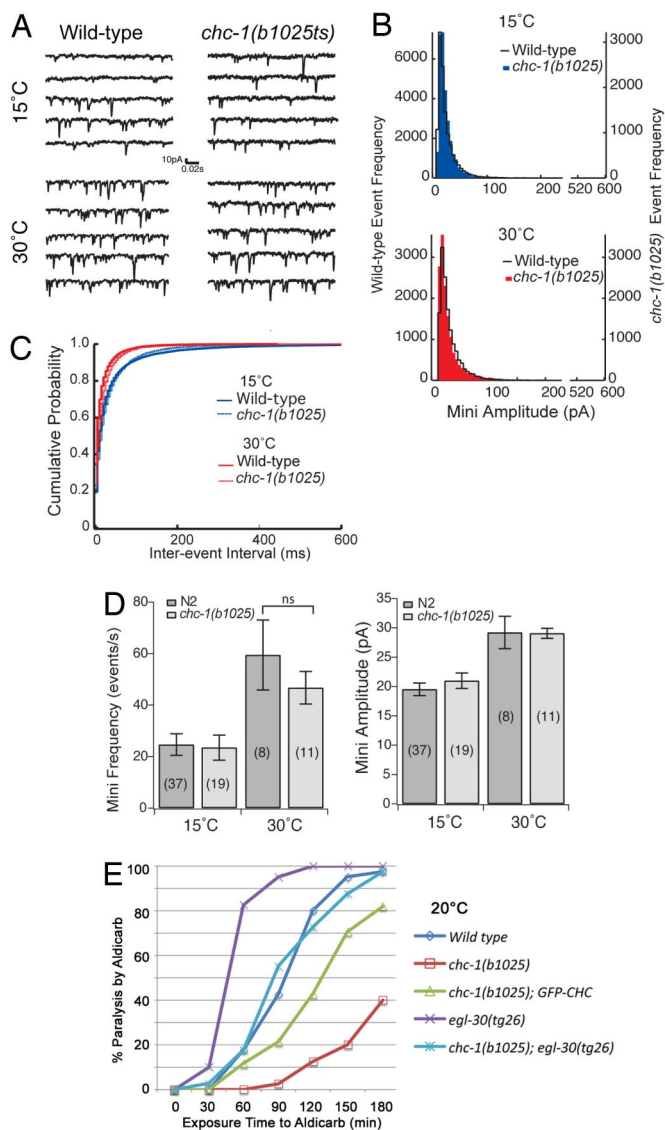


Fig. 5. Normal synaptic transmission in neurons of *chc-1(b1025ts)* animals. *chc-1(b1025ts)* mini frequency and amplitude are statistically indistinguishable from wild type at 15°C and 30°C. (A) Event records from animals raised at 15°C or animals exposed to 30°C for 1 h. (B) Histograms of pooled event mini amplitude for each genotype and condition. At 30°C a slight increase in the distributions is seen for both wild type and *chc-1(b1025ts)* (5-pA bins). (C) Cumulative probability of pooled inter-event intervals showing mini intervals decreases with increased temperature for both wild type and *chc-1(b1025ts)* (5-ms bins). (D) Quantification of average mini amplitude and frequency from individual animals from each genotype and at each condition. (E) Aldycarb sensitivity assay. Forty L4 hermaphrodites of wild-type, *chc-1(b1025ts)*, *egl-30(tg26)*, and *chc-1(b1025ts) egl-30(tg26)* animals were incubated at 15°C and then placed on aldycarb plates (0.5 mM) at 20°C. The *chc-1(b1025ts)* mutant animals expressing GFP-CHC (*dkEx6[Prgef-1::GFP::chc-1]*) under the control of a neuron-specific promoter also were examined. These animals were checked for their ability to move at the indicated time-points in response to prodding.

5). A likely remaining possibility is that probability of vesicle release is reduced in vivo, but this inhibition of release cannot be detected in a dissected preparation. Feedback inhibition, possibly mediated by acetylcholine itself through G protein-coupled metabotropic receptors (22), may be disrupted in our semi-intact preparation by superfused extracellular buffers. Inefficient receptor internalization in the clathrin mutant could lead to a build-up of inhibitory receptors on the motor neuron surface. To test whether G protein-

mediated inhibition of release could be overcome by a constitutively active stimulatory G protein, we introduced the *egl-30(tg26)* gain-of-function mutation $G\alpha_q$ into the clathrin mutant background. This mutant form of $G\alpha_q$ is known to increase the rate of acetylcholine release and confers hypersensitivity to aldycarb (23). Consistent with increasing vesicle release in the clathrin mutant background, the constitutively active $G\alpha_q$ suppressed the aldycarb resistance of *chc-1(b1025ts)* (Fig. 5E).

Discussion

Here we identify a temperature-sensitive mutant of CHC in a multicellular animal and show that clathrin is essential for receptor-mediated endocytosis and development. Although reduction of clathrin function blocks receptor-mediated endocytosis in oocytes, synaptic vesicle formation appears to be normal, albeit with altered morphology.

Several recent studies have reported that perturbing clathrin function interferes with synaptic vesicle recycling upon intense stimulation. Specifically, photoinactivation of both CLC and CHC using a fluorescein-assisted light inactivation (FIAsH-FALI) technology disrupts synaptic vesicle recycling at *Drosophila* synapses upon high stimulation (24, 25). FIAsH-FALI generates reactive oxygen species on the targeted molecule that can damage nearby molecules within a radius of at least 40 Å (26). It is possible that photolytic destruction generates protein fragments that may have antimorphic activity at the synapse. In addition, photolysis of clathrin may inactivate clathrin-interacting proteins, including regulators of membrane-associated actin assembly such as huntingtin-interacting protein 1-related protein (27, 28). Thus photolysis studies underscore the importance of clathrin-associated proteins for endocytosis of synaptic vesicles, but photolysis may in fact generate a more severe phenotype than a simple loss of clathrin.

In contrast to photoinactivation, RNAi reduces protein levels without generating protein fragments. Chronic RNAi of clathrin in hippocampal synapses causes a loss of synaptic vesicle endocytosis immediately after stimulation (29). These treated nerve terminals possessed normal levels of releasable vesicles before stimulation even though clathrin function had been disrupted for 3 d before stimulation. These data suggest that functional synaptic vesicles exist even when clathrin function has been disrupted. These data are consistent with the observations in *Drosophila*. When clathrin was photoinactivated at the fly neuromuscular junction, but synapses were not hyperstimulated, normal numbers of synaptic vesicles were observed (24), and neurotransmission was not affected upon mild stimulation (25). It is possible that an alternative mechanism for endocytosis can maintain vesicle pools when clathrin activity is impaired.

Taken together these studies indicate a surprising ability to maintain significant synaptic vesicle pools with little or no clathrin activity. This result also is consistent with mouse dynamin knockout mutants; these animals have surprisingly mild defects in synaptic transmission and synaptic vesicle number. Dynamin1 is largely dispensable for the biogenesis and endocytic recycling of synaptic vesicles; defects are most severe in inhibitory synapses, which might have very high rates of exocytosis (30, 31).

In our study we did not observe any significant defect in synaptic vesicle biogenesis in CHC mutants. Perhaps the residual clathrin (<2%) in the *chc-1(b1025ts)* animals is sufficient for the maintenance of synaptic vesicle pools in neurons under most physiological conditions. However, overexpression of the CHC-1(b1025) mutant protein cannot rescue the mutant phenotype, suggesting that the phenotype is not simply the result of the decrease in abundance of clathrin. Rather, it is more likely that the phenotype is the result of a failure of clathrin assembly and function. The mutant C termini display strongly reduced interaction at the restrictive temperature in a 2-hybrid assay, suggesting that triskelia cannot form. In fact, receptor-mediated endocytosis is severely blocked at the restrictive temperature in *chc-1(b1025ts)*, demonstrating that this mutation

severely reduces clathrin function. Together these data suggest that the mutant protein is likely to represent a loss of clathrin cage formation at high temperatures.

How can synaptic vesicles be generated with clathrin activity so diminished? In kiss-and-run recycling, synaptic vesicles are thought to fuse partially with the plasma membrane, forming a fusion pore large enough to release neurotransmitter. The synaptic vesicles then are pulled back into the cytoplasm without a need for clathrin (32, 33). This model predicts that endocytosis should take place at the active zone. A clathrin-independent mechanism that occurs at the active zone has been suggested in *Drosophila* (34). Alternatively, it is possible that clathrin is important for vesicle morphology but is not an essential component in synaptic vesicle formation. Recent studies in yeast have demonstrated that endocytosis takes place at sites enriched for clathrin and actin but that clathrin itself is not required for endocytosis at these sites (35). The large ensemble of secondary players may be capable of generating vesicles in the absence of clathrin.

Materials and Methods

General Methods and Strains. *C. elegans* strains were derived from the wild-type Bristol strain N2. Worm cultures, genetic crosses, and other *C. elegans* methods were performed according to standard protocols (36). RNAi was performed by the feeding method (37). *b1024* and *b1025* mutants were isolated in a screen described previously (6). The methods are described further in *SI Text*.

Electron Microscopy. Fixations were performed using a high-pressure freezing apparatus followed by substitution of solvent and fixative at -90°C . Two hundred fifty ultrathin (33 nm) contiguous sections were cut, and the ventral nerve cord was reconstructed from 2 animals representing each genotype.

Electrophysiology Methods. Adult animals were dissected as described previously (38) to expose the muscles of neuromuscular junctions to a patch-clamp pipette. Dissected animals were bathed in an external saline (in mM): 150 NaCl, 5 KCl, 1 MgCl₂, 5 CaCl₂, 15 Hepes, and 10 glucose (pH 7.35) and adjusted to 340 mOsm with sucrose. The pipette solution contained 120 KCl, 20 KOH, 4 MgCl₂, 5 N-Tris(hydroxymethyl)methyl-2-aminoethanesulfonic acid, 0.25 CaCl₂, 4 NaATP, 36 sucrose, 5 EGTA (pH 7.2). Pipettes were pulled and fire-polished to a tip resistance of 3–5 M Ω . Tight-seal whole-cell voltage clamp recordings of miniature current events were acquired with an EPC-10 amplifier (HEKA) in voltage-clamp mode at a holding potential of -60 mV. Analog signals were filtered at 2 kHz and sampled at 10 kHz. Events were analyzed with Mini-Analysis (Synaptosoft) with an event detection threshold 5 times the RMS baseline noise (range 1–4 pA). Animals—wild-type N2 and *chc-1(b1025ts)*—used for recordings were maintained at 15°C . Animals recorded under permissive conditions were dissected immediately and recorded in an air-conditioned room where the bath temperature averaged $20 \pm 1^{\circ}\text{C}$. Animals recorded under restrictive conditions first were pretreated by placing animals in a 30°C air incubator for 1 h. Animals then were dissected immediately in a heated room (23°C) and recorded on a warmed stage (average bath temperature of $26 \pm 2^{\circ}\text{C}$).

ACKNOWLEDGMENTS. We thank Y. Jin (University of California, San Diego), M. Zhen (Mount Sinai Hospital), M. Nonet (Washington University), and K. Schuske (University of Utah) for reagents; R. Y. Tsien (University of California, San Diego) for mRFP plasmids; and the *Caenorhabditis* Genetic Center for strains. We thank J. L. Bessereau (INSERM, France) for high-pressure freezing samples during the start of this project. We thank A. Harada and Y. Kidokoro (Gunma University, Japan) for support and discussion. This work was supported by National Institutes of Health Grants GM067237 (to B.D.G.) and NS034307 (to E.M.J.). E.M.J. is a Howard Hughes Investigator. This research was supported by the Ministry of Education, Culture, Sports, Science and Technology-Japan (MEXT) Grant-in-Aid for Scientific Research on Priority Areas 2007 (Protein Community); by Scientific Research (C), 2008; and by Bioarchitect Research Projects II of RIKEN (K.S.). This work also was supported by grants-in-aid and by the Global Center of Excellence Program from the Japanese MEXT (M.S. and K.S.).

- Brodsky FM, Chen CY, Kneuhl C, Towler MC, Wakeham DE (2001) Biological basket weaving: Formation and function of clathrin-coated vesicles. *Annu Rev Cell Dev Biol* 17:517–568.
- Heuser J (1980) Three-dimensional visualization of coated vesicle formation in fibroblasts. *J Cell Biol* 84:560–583.
- Heuser JE, Reese TS (1973) Evidence for recycling of synaptic vesicle membrane during transmitter release at the frog neuromuscular junction. *J Cell Biol* 57:315–344.
- Maycox PR, Link E, Reetz A, Morris SA, Jahn R (1992) Clathrin-coated vesicles in nervous tissue are involved primarily in synaptic vesicle recycling. *J Cell Biol* 118:1379–1388.
- Bazinnet C, Katzen AL, Morgan M, Mahowald AP, Lemmon SK (1993) The *Drosophila* clathrin heavy chain gene: Clathrin function is essential in a multicellular organism. *Genetics* 134:1119–1134.
- Grant B, Hirsh D (1999) Receptor-mediated endocytosis in the *Caenorhabditis elegans* oocyte. *Mol Biol Cell* 10:4311–4326.
- Lemmon SK, Pellicena-Palle A, Conley K, Freund CL (1991) Sequence of the clathrin heavy chain from *Saccharomyces cerevisiae* and requirement of the COOH terminus for clathrin function. *J Cell Biol* 112:65–80.
- Chen CY, Graham TR (1998) An *arf1* Δ synthetic lethal screen identifies a new clathrin heavy chain conditional allele that perturbs vacuolar protein transport in *Saccharomyces cerevisiae*. *Genetics* 150:577–589.
- Fotin A, et al. (2004) Molecular model for a complete clathrin lattice from electron cryomicroscopy. *Nature* 432:573–579.
- Poupon V, et al. (2008) Clathrin light chains function in mannose phosphate receptor trafficking via regulation of actin assembly. *Proc Natl Acad Sci USA* 105:168–173.
- Boehm M, Bonifacino JS (2001) Adaptins: The final recount. *Mol Biol Cell* 12:2907–2920.
- Hinrichsen L, Harborth J, Andrees L, Weber K, Ungewickell EJ (2003) Effect of clathrin heavy chain- and α -adaptin-specific small inhibitory RNAs on endocytic accessory proteins and receptor trafficking in HeLa cells. *J Biol Chem* 278:45160–45170.
- Liu SH, Wong ML, Craik CS, Brodsky FM (1995) Regulation of clathrin assembly and trimerization defined using recombinant triskelion hubs. *Cell* 83:257–267.
- Slepnev VI, De Camilli P (2000) Accessory factors in clathrin-dependent synaptic vesicle endocytosis. *Nature Reviews Neuroscience* 1:161–172.
- Zhen M, Jin Y (1999) The liprin protein SYD-2 regulates the differentiation of presynaptic termini in *C. elegans*. *Nature* 401:371–375.
- Murthy VN, De Camilli P (2003) Cell biology of the presynaptic terminal. *Annu Rev Neurosci* 26:701–728.
- Altun-Gultekin Z, et al. (2001) A regulatory cascade of three homeobox genes, *ceh-10*, *ttx-3* and *ceh-23*, controls cell fate specification of a defined interneuron class in *C. elegans*. *Development* 128:1951–1969.
- Salcini AE, et al. (2001) The Eps15 *C. elegans* homologue EHS-1 is implicated in synaptic vesicle recycling. *Nat Cell Biol* 3:755–760.
- Rand JB, Johnson CD (1995) Genetic pharmacology: Interactions between drugs and gene products in *Caenorhabditis elegans*. *Methods Cell Biol* 48:187–204.
- Lewis JA, Wu CH, Berg H, Levine JH (1980) The genetics of levamisole resistance in the nematode *Caenorhabditis elegans*. *Genetics* 95:905–928.
- Fatt P, Katz B (1952) Spontaneous subthreshold activity at motor nerve endings. *J Physiol (London)* 117:109–128.
- Dittman JS, Kaplan JM (2008) Behavioral impact of neurotransmitter-activated G-protein-coupled receptors: Muscarinic and GABAB receptors regulate *Caenorhabditis elegans* locomotion. *J Neurosci* 28:7104–7112.
- Doi M, Iwasaki K (2002) Regulation of retrograde signaling at neuromuscular junctions by the novel C2 domain protein AEX-1. *Neuron* 33:249–259.
- Heerssen H, Fetter RD, Davis GW (2008) Clathrin dependence of synaptic-vesicle formation at the *Drosophila* neuromuscular junction. *Curr Biol* 18:401–409.
- Kasprowitz J, et al. (2008) Inactivation of clathrin heavy chain inhibits synaptic recycling but allows bulk membrane uptake. *J Cell Biol* 182:1007–1016.
- Beck S, et al. (2002) Fluorophore-assisted light inactivation: A high-throughput tool for direct target validation of proteins. *Proteomics* 2:247–255.
- Bennett EM, Chen CY, Engqvist-Goldstein AE, Drubin DG, Brodsky FM (2001) Clathrin hub expression dissociates the actin-binding protein Hip1R from coated pits and disrupts their alignment with the actin cytoskeleton. *Traffic* 2:851–858.
- Chen CY, Brodsky FM (2005) Huntingtin-interacting protein 1 (Hip1) and Hip1-related protein (Hip1R) bind the conserved sequence of clathrin light chains and thereby influence clathrin assembly *in vitro* and actin distribution *in vivo*. *J Biol Chem* 280:6109–6117.
- Granseth B, Odermatt B, Royle SJ, Lagnado L (2006) Clathrin-mediated endocytosis is the dominant mechanism of vesicle retrieval at hippocampal synapses. *Neuron* 51:773–786.
- Ferguson SM, et al. (2007) A selective activity-dependent requirement for dynamin 1 in synaptic vesicle endocytosis. *Science* 316:570–574.
- Hayashi M, et al. (2008) Cell- and stimulus-dependent heterogeneity of synaptic vesicle endocytic recycling mechanisms revealed by studies of dynamin 1-null neurons. *Proc Natl Acad Sci USA* 105:2175–2180.
- Ceccarelli B, Hurlbut WP, Mauro A (1973) Turnover of transmitter and synaptic vesicles at the frog neuromuscular junction. *J Cell Biol* 57:499–524.
- An S, Zenisek D (2004) Regulation of exocytosis in neurons and neuroendocrine cells. *Curr Opin Neurobiol* 14:522–530.
- Kidokoro Y (2006) Vesicle trafficking and recycling at the neuromuscular junction: Two pathways for endocytosis. *Int Rev Neurobiol* 75:145–164.
- Kaksonen M, Toret CP, Drubin DG (2005) A modular design for the clathrin- and actin-mediated endocytosis machinery. *Cell* 123:305–320.
- Brenner S (1974) The genetics of *Caenorhabditis elegans*. *Genetics* 77:71–94.
- Kamath RS, Ahringer J (2003) Genome-wide RNAi screening in *Caenorhabditis elegans*. *Methods* 30:313–321.
- Richmond JE, Davis WS, Jorgensen EM (1999) UNC-13 is required for synaptic vesicle fusion in *C. elegans*. *Nat Neurosci* 2:959–964.

Supporting information

Sato et al. 10.1073/pnas.0809541106

SI Text

Additional General Methods and Strains. Strains expressing transgenes in germline cells were grown at 25 °C. Other strains were grown at 15 °C or 20 °C. Transgenic strain *bIs1* [*vit-2::GFP*] expressing a fusion of YP170, a yolk protein, and GFP was used to monitor yolk uptake by oocytes (1). A transgenic strain *nIs52*[*Punc-25::SNB-1::GFP*; *lin-15(+)*] was kindly provided by Dr. Yishi Jin at the University of California, San Diego. The other strains were obtained from *Caenorhabditis* Genetics Center. A genomic clone of clathrin light chain was amplified by PCR and subcloned into RNAi vector L4440. For RNAi knockdown, larval stage 4 (L4) worms were placed onto RNAi plates, and P0 adults or F1 progeny were subsequently scored for phenotype.

Genetic Mapping and Molecular Cloning. *b1024* was isolated using the mutator strain DH1069 *mut-7* (*pk204*); *bIs1*[*vit-2::GFP*, *rol-6* (*su1006*)]. For the isolation of the *b1025* temperature-sensitive mutant, DH1006 *bIs1*[*vit-2::GFP*, *rol-6* (*su1006*)] was mutagenized with *N*-ethyl-*N*-nitrosourea, and the F₁ and F₂ generations were grown at 15 °C. After incubation at 25 °C for 12–24 h, the F₂ generation was screened for animals exhibiting little or no GFP signal in oocytes and embryos but showing bright GFP signal in body cavity. Both *rme-3* mutations are recessive. The *rme-3* mutations were mapped to the middle of LGIII by SNP mapping (2). To identify a candidate for *rme-3*, we surveyed predicted genes in the *C. elegans* genomic sequence in this region and found *chc-1* (T20G5.1). RNAi of *chc-1* was known to produce a strong receptor-mediated endocytosis (RME) phenotype and severe embryonic lethality. Expression of GFP-CHC-1 complemented the temperature-sensitive embryonic lethality of *rme-3*(*b1025ts*). Genomic regions from *chc-1* were amplified from each *rme-3* mutant by PCR for sequencing.

Plasmids and Transgenic Strains. We used the *bIs5*[*GFP::chc-1*, *rol-6(d)*] strain expressing GFP-CHC-1 under the control of the *chc-1* promoter for complementation testing (3). For cell-specific expression we cloned the *chc-1* ORF into Gateway destination vectors (Invitrogen). Genomic DNAs containing the ORFs of *chc-1*(+) and *chc-1*(*b1025ts*) were amplified by PCR and cloned into the Entry vector pDONR221. To drive expression of the GFP-fusion genes in the maternal germ line, we used a destination vector pID3.01B, which contains *pie-1* 5' UTR-GFP-Gateway cassette-*pie-1* 3' UTR sequences with the cotransformation marker *C. elegans unc-119* (4). The ORF of *chc-1* or *chc-1*(*b1025*) in pDONR221 then was transferred into pID3.01B by Gateway recombination cloning technology. These plasmids were introduced into *unc-119*(*ed3*) by microparticle bombardment (5) to generate the integrants *pwIs47*[*Ppie-1::GFP::chc-1*] and *pwIs96*[*Ppie-1::GFP::chc-1*(*b1025ts*)].

For intestinal expression of transgenes, we used a destination vector containing the *vha-6* promoter-GFP-Gateway cassette-*let-858* terminator with *C. briggsae unc-119* (6). For expression of the transgenes in GABA neurons, we constructed a Gateway destination vector pKS7, which contains the *unc-25* promoter-mRFP-Gateway cassette-*let-858* terminator with *C. briggsae unc-119*. The ORF of *chc-1* or *chc-1*(*b1025*) on pDONR221 was transferred into these vectors by Gateway recombination cloning technology. These plasmids were introduced into *unc-119*(*ed3*) by the bombardment method to generate the integrants *dkIs8*[*Pvha-6::GFP::chc-1*], *dkIs14*[*Pvha-6::GFP::chc-1*(*b1025*)] and *pwIs122*[*Punc-25::mRFP::chc-1*].

For pan-neuronal expression of *N*-terminal GFP fusion protein,

we constructed a destination vector, pKS12, which contains *rgef-1*/*F25B3.3* promoter, followed by GFP, a Gateway cassette, and the transcriptional *let-858* terminator. The *chc-1* ORF was transferred into pKS12 and microinjected into *chc-1*(*b1025ts*). This strain was used to examine complementation of the thrashing defect of *chc-1*(*b1025ts*) by neuron-specific expression of CHC-1. We also created a strain expressing GFP-CHC-1 in GABA neurons under *unc-47* promoter control, *oxIs164*[*Punc-47::GFP::chc-1*] by the microinjection method for colocalization analysis.

Western Blotting. To examine the amount of endogenous CHC-1, α -adaptin, and RME-1, 50 adult hermaphrodites were incubated at 15 °C or 25 °C and subjected to Western blotting as described previously (1). To determine the amount of GFP-CHC-1 proteins, 80 adult hermaphrodites expressing GFP-CHC-1 or GFP-CHC-1(*b1025*) under the control of *vha-6* promoter were incubated at 15 °C, 25 °C, or 30 °C and subjected to Western blotting. Rabbit anti-CHC polyclonal antibody, rabbit anti- α -adaptin polyclonal antibody, and rabbit anti-RME-1 polyclonal antibody were used as described previously (5, 7, 8). Rat anti-GFP monoclonal antibody (GF090R) was purchased from NACARA-RAI tesque, Inc. and used at a 1:500 dilution.

Microscopy and Immunostaining. Fluorescence images were obtained using an Axiovert 200M (Carl Zeiss MicroImaging, Inc.) microscope equipped with a digital CCD camera (C4742–95-12ER, Hamamatsu Photonics) and deconvolved with AutoDeblur software (AutoQuant Imaging Inc.). Confocal images were obtained using an Olympus confocal microscope system FV1000 (Olympus Corp.). Examination of images was performed with Metamorph software (Universal Imaging Co). To observe live worms expressing transgenes, worms were mounted on agarose pads with 10 mM levamisole in M9 buffer. Immunostaining of dissected gonads was performed as described previously (1). Whole-mount immunofluorescent staining of neurons was performed as described (9). Anti-SYD-2 polyclonal antibody was kindly provided by Dr. Mei Zhen of the University of Toronto. Mouse anti-GFP monoclonal antibody (3E6), Alexa Fluor 488-conjugated goat anti-mouse IgG, and Alexa Fluor 568-conjugated goat anti-rabbit IgG were obtained from QBIogene Inc. and Molecular Probes Corporation, respectively. For immunostaining of RAB-3, SNT-1, SNB-1, and UNC-64, animals were fixed and prepared for immunocytochemistry using a modified Bouin's fixative or 2% paraformaldehyde (10, 11). The following antibodies were used: mouse anti-RAB-3 (11), rabbit anti-synaptotagmin (SNT-1) (10), rabbit anti-synaptobrevin (SNB-1) (12), rabbit anti-UNC-64 (13), and mouse GFP; (Roche Applied Science). Appropriate secondary Alexa Fluor 488 and Alexa Fluor 555-conjugated antibodies were used (Molecular Probes).

Immunostaining of dissected gonads were performed as described previously (1). The following antibodies were used: rabbit anti-CHC polyclonal antibody (8), rabbit anti- α -adaptin polyclonal antibody (5), and mouse anti-GFP (Roche Applied Science). Appropriate secondary Alexa Fluor 488 and Alexa Fluor 555-conjugated antibodies were used (Molecular Probes).

Thrashing movies were made using PixelINK capture software and a PixelINK PL-A661 firewire CCD camera attached to 10 \times ocular of an Olympus dissecting microscope.

Thrashing Assay. The thrashing assay was used to investigate the frequency of contraction of body-wall muscles in worms. L4 hermaphrodites of wild-type (N2) and *chc-1* mutant worms were

grown synchronously to the young adult stage at 15 °C, 20 °C, or 25 °C. For 30 °C incubation, L4 hermaphrodites were grown at 15 °C for 24 h to the young adult stage and then transferred onto a 30 °C pre-warmed OP50-seeded NGM (normal growth medium) plate. These worms were transferred into 200 μ l of 15 °C, 20 °C, 25 °C, or 30 °C pre-warmed M9 buffer on a depression slide to count their thrashes for 3 min. A thrash is defined as a change in the direction with the body bending in the middle.

Pharmacological Assays. Resistance of wild-type and mutant worms to aldicarb was performed as described (14). Briefly, young adult animals were placed on plates containing 0.5 mM aldicarb and assayed for paralysis at 30-min or 60-min intervals over a 3-h time-period indicated by a lack of response upon poking with a metal wire. To test for sensitivity to levamisole, 30 young adult hermaphrodites were placed on levamisole plates (60 μ M), and their movement was checked by poking. *lev-1(e211)* was used as a control of aldicarb and levamisole resistance. The number of paralyzed worms was counted at different time-points following exposure to aldicarb or levamisole, and the data were analyzed as the percent of animals that were paralyzed at each time-point.

Electron Microscopy. Fixations were performed using a high-pressure freezing apparatus followed by substitution of solvent and fixative at -90 °C. For animals raised at the permissive temperature in experiment #1 (See supporting information (SI) Table S2), broods of wild-type and *chc-1(b1025ts)* worms were maintained at 15 °C and were exposed to ambient temperature for less than 2 min; in experiment #2, mutant worms were exposed to ambient temperature for less than 10 min. Note that 10-min exposure to room temperature was sufficient to change the diameter of synaptic vesicles. For animals raised at the nonpermissive temperature, animals in experiment #1 were raised at 15 °C and incubated at 30 °C for 2 h before freezing; animals in experiment #2 were raised at 15 °C and incubated at 25 °C for 24 h before freezing. Fixations were performed for the most part as described previously (15). Briefly, 10 animals were placed into a freeze chamber (a 100- μ m well of a type A specimen carrier) containing space-filling bacteria, covered with a type B specimen carrier flat side down, and frozen instantaneously in the BAL-TEC HPM 010 (BAL-TEC). Then, the frozen animals were fixed in a Leica EM AFS system with 0.5% glutaraldehyde and 0.1% tannic acid in anhydrous acetone for 4 days at -90 °C, followed by 2% osmium tetroxide in anhydrous acetone for 39 h with gradual temperature increase (held at

constant temperature at -90 °C for 7 h, increased by 5 °C/h to -25 °C over 13 h, held at constant temperature at -25 °C for 16 h, and raised by 10 °C/h to 4 °C over 2.9 h). The fixed animals were embedded in araldite resin following the infiltration series (30% araldite/acetone for 4 h, 70% araldite/acetone for 5 h, 90% araldite/acetone overnight, and pure araldite for 8 h). Mutant and control blocks were blinded. Ribbons of ultrathin (33 nm) serial sections were collected using an Ultracut E microtome (Leica). Images were obtained on a Hitachi H-7100 electron microscope using a Gatan slow-scan digital camera (Gatan). Two hundred fifty ultrathin (33 nm) contiguous sections were cut, and the ventral nerve cord was reconstructed from 2 animals representing each genotype. Image analysis was performed using Image J software (National Institutes of Health). The numbers of synaptic vesicles (~ 30 nm), dense-core vesicles (~ 40 nm), and large vesicles (>40 nm) in each synapse were counted, and their distance from presynaptic specialization and plasma membrane and the diameter of each was measured from the cholinergic neurons VA and VB and the GABA neuron VD. Genotypes were unblinded only after completion of the morphometric analysis.

Additional Electrophysiology Methods. To warm the stage, a method commonly used by mammalian cell biologists to maintain cells at elevated temperatures was used (16). Briefly, warm air from a hair dryer was directed through heating duct to the underside of the microscope stage. The distance of the end of the duct from the stage controls the stage temperature. This method of heating the stage did not introduce electrical or mechanical noise and was stable for the duration of the recording. Bath temperature was monitored by a thermistor probe inserted in the bath and read out on a Warner TC-324B temperature display.

Two-Hybrid Assay. The DupLEX-A 2-hybrid system (OriGene Technologies, Inc.) was used according to manufacturer's instructions. A cDNA fragment corresponding to the C-terminal hub region of CHC-1 (residues 1075–1680) or CHC-1(b1025) was cloned into pEG202 (the bait vector) and pJG4–5 (the prey vector). These plasmids were introduced into reporter strains EGY48 or EGY194 included with the system. To assess the expression of the *LEU2* reporter, transformants were grown on plates lacking leucine, histidine, tryptophan, and uracil and containing 2% galactose/1% raffinose at 30 °C or 37 °C for 3 days. The amount of the expressed protein in each yeast cell lysate (30 μ g) was estimated by Western blotting using rat anti-HA monoclonal antibody 3F10 (Roche Applied Science).

- Grant B, Hirsh D (1999) Receptor-mediated endocytosis in the *Caenorhabditis elegans* oocyte. *Mol Biol Cell* 10:4311–4326.
- Wicks SR, Yeh RT, Gish WR, Waterston RH, Plasterk RH (2001) Rapid gene mapping in *Caenorhabditis elegans* using a high density polymorphism map. *Nat Genet* 28:160–164.
- Greener T, et al. (2001) *Caenorhabditis elegans* auxilin: a J-domain protein essential for clathrin-mediated endocytosis *in vivo*. *Nat Cell Biol* 3:215–219.
- Pellettieri J, Reinke V, Kim SK, Seydoux G (2003) Coordinate activation of maternal protein degradation during the egg-to-embryo transition in *C. elegans*. *Dev Cell* 5:451–462.
- Sato M, et al. (2005) *Caenorhabditis elegans* RME-6 is a novel regulator of RAB-5 at the clathrin-coated pit. *Nat Cell Biol* 7:559–569.
- Chen CC, et al. (2006) RAB-10 is required for endocytic recycling in the *C. elegans* intestine. *Mol Biol Cell* 17:1286–1297.
- Grant B, et al. (2001) Evidence that RME-1, a conserved *C. elegans* EH-domain protein, functions in endocytic recycling. *Nat Cell Biol* 3:573–579.
- Sato M, et al. (2008) Regulation of endocytic recycling by *C. elegans* Rab35 and its regulator RME-4, a coated-pit protein. *EMBO J* 27:1183–1196.
- Zhen M, Jin Y (1999) The liprin protein SYD-2 regulates the differentiation of presynaptic termini in *C. elegans*. *Nature* 401:371–375.
- Nonet ML, Grundahl K, Meyer BJ, Rand JB (1993) Synaptic function is impaired but not eliminated in *C. elegans* mutants lacking synaptotagmin. *Cell* 73:1291–1305.
- Nonet ML, et al. (1997) *Caenorhabditis elegans* rab-3 mutant synapses exhibit impaired function and are partially depleted of vesicles. *J Neurosci* 17:8061–8073.
- Nonet ML, Saifee O, Zhao H, Rand JB, Wei L (1998) Synaptic transmission deficits in *Caenorhabditis elegans* synaptobrevin mutants. *J Neurosci* 18:70–80.
- Saifee O, Wei L, Nonet ML (1998) The *Caenorhabditis elegans* *unc-64* locus encodes a syntaxin that interacts genetically with synaptobrevin. *Mol Biol Cell* 9:1235–1252.
- Miller KG, et al. (1996) A genetic selection for *Caenorhabditis elegans* synaptic transmission mutants. *Proc Natl Acad Sci USA* 93:12593–12598.
- Rostaing P, Weimer RM, Jorgensen EM, Triller A, Bessereau JL (2004) Preservation of immunoreactivity and fine structure of adult *C. elegans* tissues using high-pressure freezing. *J Histochem Cytochem* 52:1–12.
- Dailey M (2000) Maintaining live cells and tissue slices in the imaging setup. *Imaging Neurons: A Laboratory Manual* (Cold Spring Harbor Laboratory Press, Cold Spring Harbor, MA):10.11–10.17.

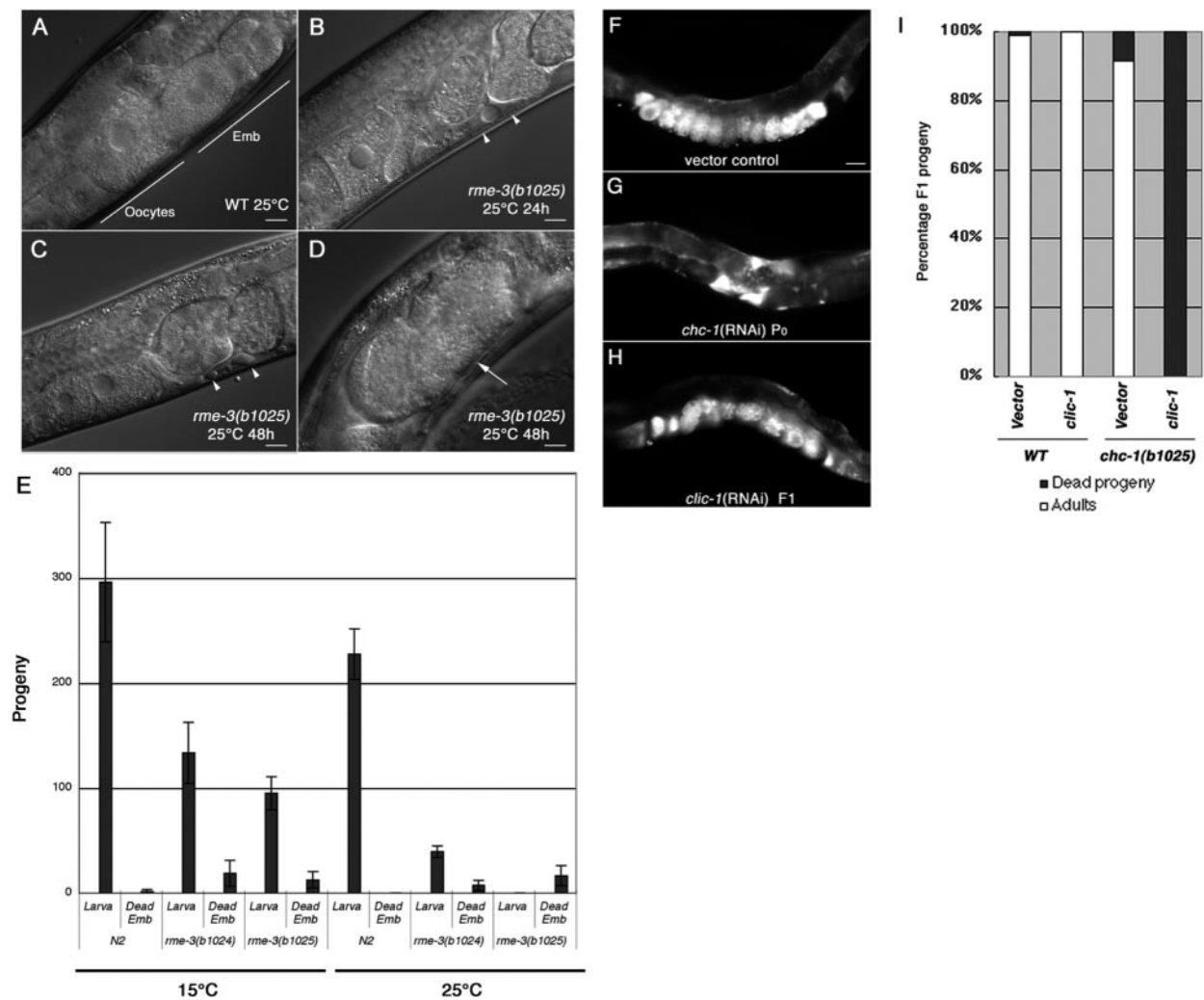


Fig. S1. (A–D) Clathrin is essential for embryogenesis and development. After incubation at 25°C for 24 h or 48 h, *rme-3/chc-1(b1025ts)* animals accumulated yolk in the body cavity (arrowheads, B, C). In addition, embryonic debris was often found in the uterus (arrow, D). (Scale bars, 10 μ m.) (E) Progeny number in wild type (N2) and *chc-1* mutants. L4 larvae were incubated at 15°C and 25°C, and the number of larvae and dead embryos in the next generation were counted. *rme-3(b1025ts)* produced progeny at 15°C but not at 25°C. Even at the permissive temperature of 15°C, *chc-1(b1025ts)* mutant worms ($n = 4$) produced a reduced number of embryos (108 ± 23 embryos) compared with the wild-type ($n = 4$, 297 ± 56 embryos). *chc-1(b1025ts)* hermaphrodites ($n = 4$) transferred from 15°C to 25°C during the L4 stage progressed to adulthood but accumulated yolk in the body cavity and produced only dead embryos (16.5 ± 9 dead embryos/adult). Eighty-eight percent of *chc-1(b1025ts)* embryos raised at 15°C hatched and displayed normal development. However, if freshly laid *chc-1(b1025ts)* embryos ($n = 119$) were shifted to 25°C, none hatched. When *chc-1(b1025ts)* L1 larvae ($n = 66$) were shifted to 25°C, 85% were arrested during the early larval stages, and only 12% progressed to adulthood. Adults became sluggish within 10 min after transfer to 30°C. Adults maintained at 25°C died within 3 to 4 days. These data suggest that CHC is required for the functions of differentiated cells in addition to being a requirement during development. (F–H) The effects of RNAi-based gene knockdown of *chc-1* and *clic-1* on yolk uptake by oocytes. YFP170-GFP uptake by oocytes was examined in (F) a control, (G) *chc-1* (RNAi), and (H) *clic-1* (RNAi) worms at 20°C. Scale bar represents 30 μ m. (I) The phenotypic effects of *clic-1* (RNAi) in wild-type or *chc-1(b1025ts)* mutant backgrounds were assayed at 15°C. L4 larva of wild type (WT, $n = 2$) and *chc-1(b1025ts)* worms ($n = 4$) were placed on RNAi plates and the phenotype of F1 progeny was scored. RNAi of *clic-1* caused fully penetrant lethality in the *chc-1(b1025ts)* strain (total 339 dead embryos, 2 L1 arrested larva, no adults from 4 worms).

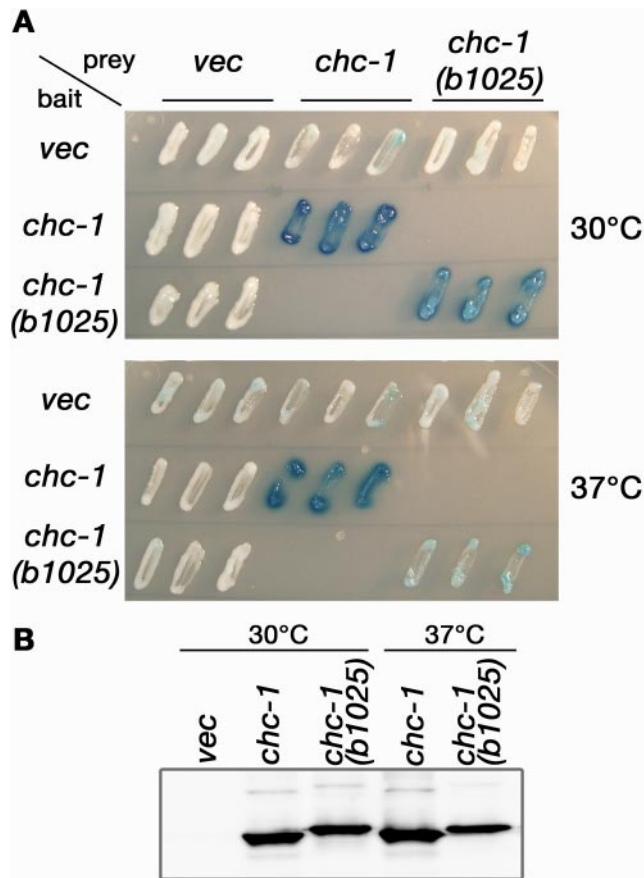


Fig. S3. Interaction of CHC-1(b1025) hub domains is impaired at high temperature. (A) A yeast 2-hybrid assay between the C-terminal hub domains of CHC-1 or CHC-1(b1025). The C-terminal hub region of CHC-1 (residues 1075–1680) or CHC-1(b1025) was expressed in a yeast reporter strain as fusions with the transcriptional activation domain of B42 (prey) or the DNA binding domain of LexA (bait). Interaction between bait and prey was tested at 30 °C (permissive temperature) and 37 °C (restrictive temperature) using β -galactosidase reporter assays. The wild-type CHC-1 hub domains interacted with each other at 30 °C and 37 °C. However, the hub domains of CHC-1(b1025) showed reduced interaction compared with wild type at 30 °C and was reduced further at 37 °C. (B) The amount of the expressed protein in each yeast cell was estimated by Western blotting using an anti-HA antibody. The expression level of the CHC-1(b1025) mutant hub domains was nearly identical to that of the wild-type CHC-1 hubs.

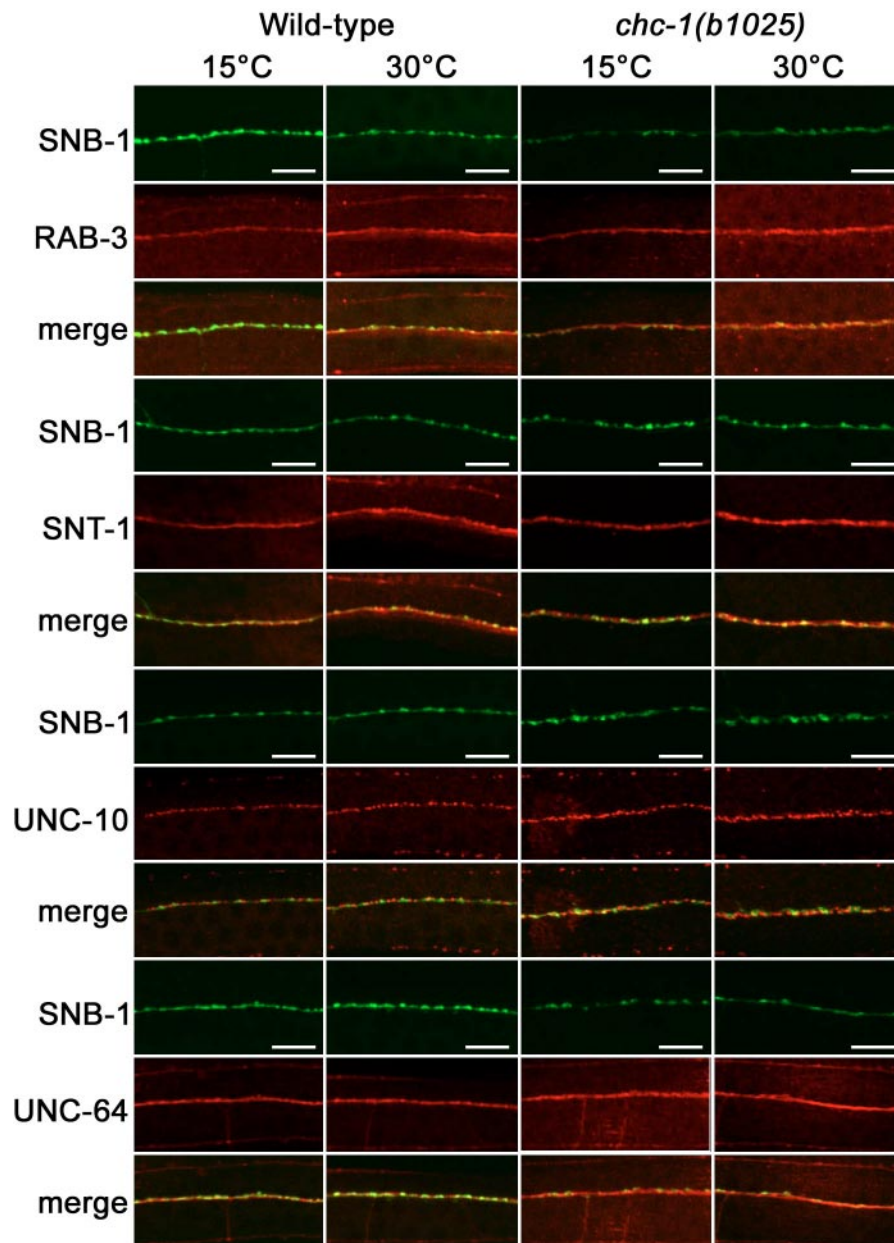


Fig. S6. Subcellular localization of synaptic proteins is unchanged in *chc-1(b1025ts)* animals. Transgenic worms expressing the synaptic vesicle protein GFP-SNB-1 in GABA neurons were stained with anti-GFP and anti-RAB-3, anti-SNT-1 (synaptotagmin), anti-UNC-10 (active zone protein), or anti-UNC-64 (syntaxin) antibodies. The localization of these synaptic proteins was largely unchanged in *chc-1(b1025ts)* mutants even at restrictive temperature. (Scale bars, 10 μ m.)

wild type @ 30°C neuromuscular junctions

chc-1(b1025) @ 30°C neuromuscular junctions

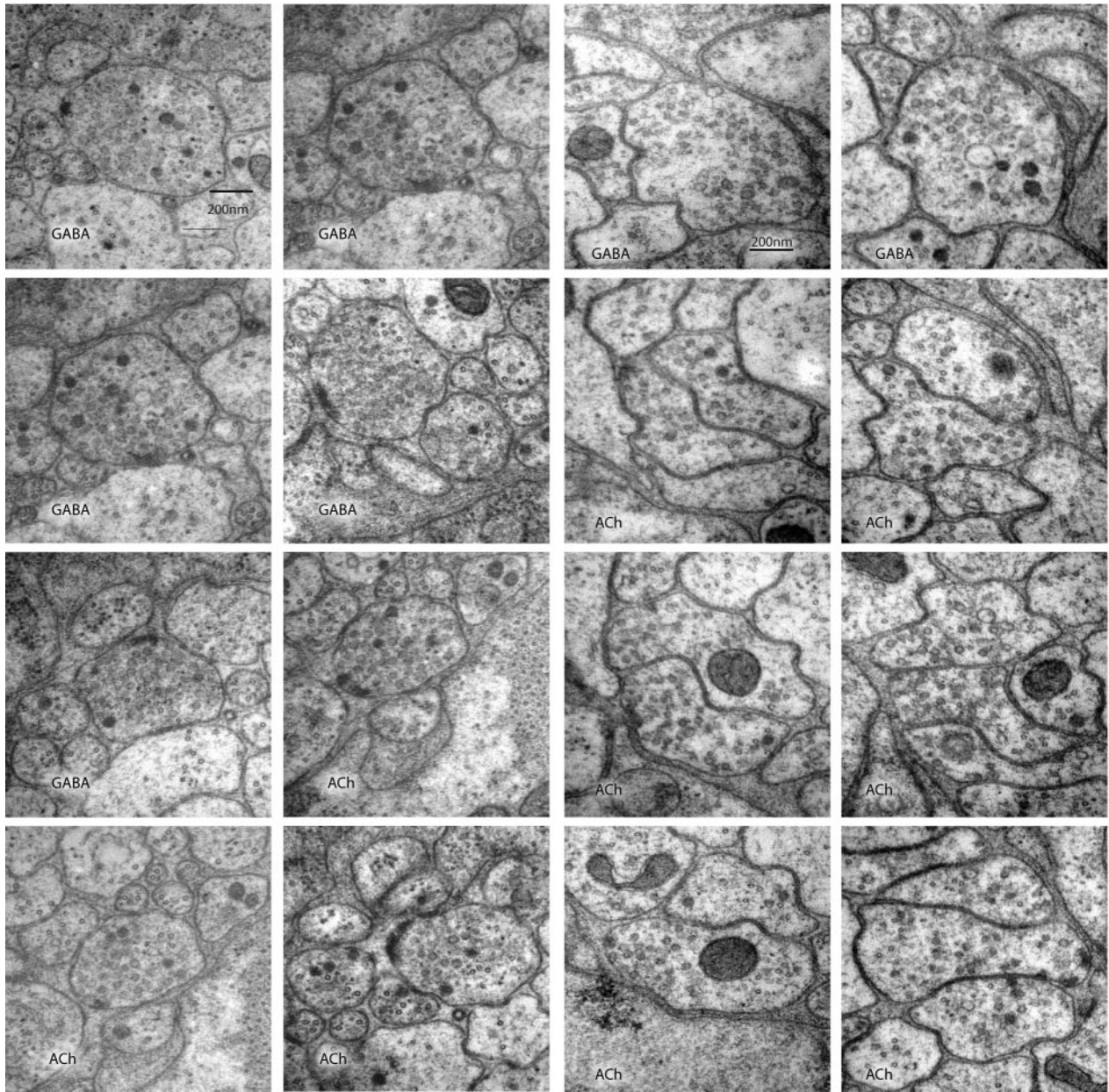
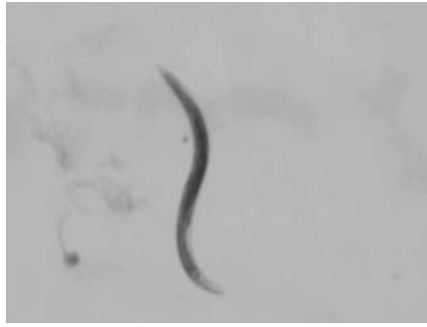


Fig. S7. Representative images of neuromuscular junctions. (Left) Wild-type adult hermaphrodites at 30°C. (Right) *chc-1(b1025ts)* adult hermaphrodites at 30°C.



Movie S1. Thrashing of wild-type and *chc-1(b1025ts)* worms. L4 larvae of wild-type (Movie S1) and *chc-1(b1025ts)* (Movie S2) worms were incubated at 25 °C for 24 h and transferred into a pre-warmed M9 buffer. Movies show worm behavior between 15 sec and 35 sec after transfer to buffer.

[Movie S1 \(MOV\)](#)

**Table S1. Pharyngeal pumping assay: pharyngeal pumps/min
(n = 8)**

Genotype	15°C	25°C
Wild-type	290 ± 7	313 ± 9
<i>chc-1(b1024)</i>	237 ± 8	227 ± 30
<i>chc-1(b1025ts)</i>	243 ± 12	166 ± 24
<i>chc-1(b1025ts) GFP-CHC-1</i>	N.T.	302 ± 12

Although the pharynx pumps at basal rates in the absence of neuronal input, pharyngeal muscle contraction is greatly stimulated by cholinergic motor neurons. Wild-type animals pump rapidly in the presence of food. The weak mutant *chc-1(b1024)* exhibited a slight defect in pharyngeal pumping at either temperature. In contrast, the temperature-sensitive mutant *chc-1(b1025ts)* exhibited a slight defect at 15°C, but pumping was reduced to half the normal rate compared with the wild type when incubated at 25°C for 24 h. The residual ability of the *chc-1* mutants in pharyngeal pumping may be caused by clathrin-independent peptidergic secretion or reflect the neuronal input-independent contraction ability of the pharynx. Neuronal expression of *GFP-CHC-1* rescued the pharyngeal pumping ability of the *chc-1(b1025ts)* mutants at 25°C. These data indicate that there is a neuronal defect in the pharynx of clathrin mutants.

Table S2. Clathrin mutants display reduced synaptic vesicle (SV) diameter but normal synaptic vesicle number

Genotype	Temperature	SV/ACh Profile	No. n = synapses/no. worms	Mean SV diameter	No. n = SV	SV/GABA profile	n = No. synapses/no. worms	Mean SV diameter	No. SV
Experiment 1									
Wild type	15°C	24 ± 2	11/2	28.2	788	40 ± 4	9/2	27.5	1369
<i>chc-1(b1025ts)</i>	15°C	24 ± 2	10/2	27.9	841	43 ± 2	9/2	27.7	1170
Wild type	30°C	25 ± 3	8/2	27.6	444	39 ± 1	8/2	27.5	718
<i>chc-1(b1025ts)</i>	30°C	22 ± 3	9/2	23.4	641	36 ± 5	8/2	24.1	730
Experiment 2									
Wild type	15°C	22 ± 2	5/1	29.3	475	28 ± 2	4/1	28.9	381
<i>chc-1(b1025ts)</i>	15°C	16 ± 2	5/1	24.1	319	22 ± 4	4/1	24.7	383
Wild type	25°C	25 ± 1	5/1	27.7	367	31 ± 2	4/1	27.5	397
<i>chc-1(b1025ts)</i>	25°C	16 ± 1	4/1	24.5	301	25 ± 2	4/1	25.6	234
Wild type	25°C thrashed	16 ± 1	4/1	27.2	275	25 ± 2	4/1	27.1	415
<i>chc-1(b1025ts)</i>	25°C thrashed	16 ± 1	4/1	24.0	224	21 ± 1	4/1	24.7	387

For synaptic vesicle numbers per synaptic profile, the *p* value was examined by Student's *t*-test where *n* = synapses examined in experiment #1:: (ACh: N2 15°C vs. *chc-1(b1025ts)* 15°C, *P* = 0.92; N2 15°C vs. N2 30°C, *P* = 0.80; N2 30°C vs. *chc-1(b1025ts)* 30°C, *P* = 0.46; *chc-1(b1025ts)* 15°C vs. *chc-1(b1025ts)* 30°C, *P* = 0.45); (GABA: N2 15°C vs. *chc-1(b1025ts)* 15°C, *P* = 0.44; N2 15°C vs. N2 30°C, *P* = 0.91; N2 30°C vs. *chc-1(b1025ts)* 30°C, *P* = 0.52; *chc-1(b1025ts)* 15°C vs. *chc-1(b1025ts)* 30°C, *P* = 0.18). In experiment #2 there is a visible decrease in the synaptic vesicle number in *chc-1(b1025ts)* strains vs. the wild type. However, when combined with the experiment #1 data set, there is not a statistically significant difference between the genotypes: (ACh: N2 permissive vs. *chc-1(b1025ts)* permissive, *P* = 0.49; N2 restrictive vs. *chc-1(b1025ts)* restrictive, *P* = 0.97); (GABA: N2 permissive vs. *chc-1(b1025ts)* permissive, *P* = 0.95; N2 restrictive vs. *chc-1(b1025ts)* restrictive, *P* = 0.21). For synaptic vesicle diameters, the *p* value was examined by Student's *t*-test where *n* = mean diameter of vesicles in a profile: (N2, 15°C vs. *chc-1(b1025ts)*, 15°C, *P* = 0.99; N2, 15°C vs. N2, 30°C, *P* = 0.31; N2, 30°C vs. *chc-1(b1025ts)*, 30°C, *P* < 0.0001; *chc-1(b1025ts)*, 15°C vs. *chc-1(b1025ts)*, 30°C, *P* < 0.0001).